Hindawi
Advances in Meteorology
Volume 2018, Article ID 9287249, 12 pages
https://doi.org/10.1155/2018/9287249

Research Article

Carbon Exchange between the Atmosphere and a Subtropical Evergreen Mountain Forest in Taiwan

Falk Maneke-Fiegenbaum,[1] **Otto Klemm**,[1] **Yen-Jen Lai**,[2] **Chih-Yuan Hung**,[2] **and Jui-Chu Yu**[2]

[1]*Climatology Working Group-Institute of Landscape Ecology, University of Münster, 48149 Münster, Germany*
[2]*Experimental Forest, National Taiwan University, 55750 Nantou, Taiwan*

Correspondence should be addressed to Yen-Jen Lai; alanlai@ntu.edu.tw

Received 18 June 2018; Revised 16 October 2018; Accepted 24 October 2018; Published 21 November 2018

Academic Editor: Gabriele Buttafuoco

Tropical, temperate, and boreal forests are the subject of various eddy covariance studies, but less is known about the subtropical region. As there are large areas of subtropical forests in the East Asian monsoon region with possibly high carbon uptake, we used three years (2011–2013) of eddy covariance data to estimate the carbon balance of a subtropical mountain forest in Taiwan. Two techniques of flux partitioning are applied to evaluate ecosystem respiration, thoroughly evaluate the validity of the estimated fluxes, and arrive at an estimate of the yearly net ecosystem exchange (NEE). We found that advection is a strong player at our site. Further, when used alone, the nighttime flux correction with the so-called u^* method (u^* = friction velocity) cannot avoid underestimating the nighttime respiration. By using a two-technique method employing both nighttime and daytime parameterizations for flux corrections, we arrive at an estimate of the three-year mean NEE of −561 (±standard deviation 114) $g{\cdot}C{\cdot}m^{-2}{\cdot}yr^{1}$. The corrected flux estimate represents a rather large uptake of CO_2 for this mountain cloud forest, but the value is in good agreement with the few existing comparable estimates for other subtropical forests.

1. Introduction

There are complex interactions at play between earth's climate and the global forests. For example, properties and processes of the forests such as the albedo, the evapotranspiration, and the carbon cycle are relevant climate drivers and thus have an impact on climate change arising from anthropogenic greenhouse gas emission [1]. For the purpose of studying the carbon cycle of forests, there are hundreds of eddy covariance stations worldwide to quantify the atmosphere-biosphere fluxes of CO_2 [2]. Tropical, temperate, and boreal forests are the subject of numerous eddy covariance studies [3], but less is known about the subtropical region. The quantification of CO_2 fluxes in the subtropical regions is, however, very important for global change studies because these forests—which make up large areas in the East Asian monsoon region (latitude 20–40°N, longitude 100–145°E) [4]—potentially play important roles in the global carbon cycle. Integration of existing eddy covariance studies of subtropical forests in the East Asian monsoon region indicates a high carbon uptake in this region, $-362 \pm 39\ g{\cdot}C{\cdot}m^{-2}{\cdot}yr^{-1}$ [4]. However, for Taiwan, as part of this region, there are only few studies analysing the CO_2 flux in subtropical forests [5, 6]. These studies analyse processes contributing to the CO_2 fluxes, but they rely only on short experimental periods of a few weeks each, so that annual budgets cannot be derived from these data. With this study, we want to contribute to filling this gap. The aim is to quantify the yearly CO_2 uptake of a subtropical mountain cloud forest in Taiwan and put it into context with other published data.

It is well accepted that the eddy covariance technique is most suitable for quantifying CO_2 fluxes for sites with long fetches, flat terrain, and an overall very homogenous surface [7]. It is, however, a challenge to obtain reliable estimates of yearly carbon uptake by photosynthesis in mountainous

forests. Ever-present problems with the eddy covariance approach, such as advection fluxes, temporal storage of air masses within the vegetation, and stably stratified boundary layers, are even more difficult to handle in forests and complex terrain than in flat, homogenously vegetated landscapes. Nevertheless, upon the background of climate change and efforts to mitigate the net emission fluxes of greenhouse gases, it seems critical to investigate the CO_2 fluxes of these forests.

This study is based on a three-year (2011–2013) data set of eddy covariance measurements of CO_2 fluxes above a subtropical mountain forest in Taiwan. For the investigation of the yearly CO_2 net ecosystem exchange (NEE), a detailed analysis of the quality of the measured fluxes is performed. The local meteorology is analysed in detail, and the contribution of the ecosystem respiration to NEE is estimated by using a combination of several flux partitioning techniques. Finally, we develop an improved estimate of the annual carbon uptake of the subtropical forest in complex terrain by including the best estimate of ecosystem respiration into the carbon balance evaluation.

2. Materials and Methods

2.1. Site Description. This study is conducted in the Xitou tract of the Experimental Forest, National Taiwan University, located in the Nantou County, Central Taiwan. The whole forest site has an area of 2,400 ha. Today, about 620 ha are covered by natural hardwood forests [8]. The remaining area has been replaced by plantations of mostly coniferous trees which include Japanese cedar (*Cryptomeria japonica*), Taiwania (*Taiwania cryptomerioides*), Taiwan red cypress (*Chamaecyparis formosensis*), China fir (*Cunninghamia lanceolata*), and Luanta fir (*Cunninghamia konishii*) [8]. The climate in the Xitou area is dominated by a relatively dry season from October to April and a wet season from May to September. The mean annual precipitation is 2,635 mm. The mean annual temperature is 16.6°C, the maximum monthly mean is 20.8°C in July, and the minimum is 12.0°C in January. The mean relative humidity at Xitou exceeds 80%.

The experimental tower XT00 (23°39′52.7″N; 120°47′44.5″E, 1267 m above mean sea level) is located on an incline with a mean slope of 9.4° from south-southwest to north-northeast. The incline lies within complex terrain with higher mountains to the south and east (Figure 1). The tower is surrounded by a plantation composed of Japanese cedars planted in the 1950s; the stand extends up to 500 m north and over 500 m south from the experimental tower site. The plantation had a relatively even canopy height with a mean of 28 m in 2013. The mean diameter at breast height is 35 cm. The tree density is 721 trees ha^{-1}, and the mean annual increment of live-tree biomass in the immediate neighbourhood of the tower, as computed from forest inventory, is 560 $g{\cdot}C{\cdot}m^{-2}{\cdot}yr^{-1}$ (mean by linear interpolation of 2011–2017 data). In the northwest, there are patches of Taiwania, while in the southeast, there are patches of Taiwan red cypress. There are also smaller stands of bamboo forest (north) and broadleaf forest (northeast). Since the change in forest politics in Taiwan in the 1990s, there has been little forest management, and the former plantation mostly grows without disturbance.

The site has a distinct mountain-valley wind regime with valley breeze from north-northeast in the daytime and mountain breeze from south-southeast during the nighttime. Associated with the wind regime, fog occurs frequently at Xitou. It typically forms with the development of the valley breeze in the mornings. Fog is mostly frequent in the afternoons with a peak in frequency during the late afternoon hours. Over the year, the wet spring and summer seasons have the highest fog frequencies [9].

2.2. Tower, Instrumentation and Data Processing. This study used two eddy covariance systems mounted on XT00 at a 40 m (system 1) and a 32 m (system 2) height above ground level (agl), respectively. Each eddy covariance system consists of a 3D ultrasonic anemometer (Campell Scientific USA) and an open path CO_2 and H_2O gas analyser (LICOR 7500, Licor USA). The signals of the ultrasonic anemometers and the CO_2 and H_2O analysers were logged with 10 Hz temporal resolution on a Campbell CR3000 data logger. The tower is also equipped with a CO_2 and H_2O mixing ratio profile system (Licor LI-840; at heights of: 0.1, 0.5, 1, 2, 4, 8, 16, 25, 30, and 35 m agl) and a 2D wind profile system (Gill WS4 ultrasonic anemometers in the heights 6, 18, 25, 32, and 36 m agl.). Further, net radiometers are mounted at 40 m (Kipp & Zonen CNR4), 12 m, and 35 m (Kipp & Zonen NR-Lite). The photosynthetic active radiation (PAR) is measured at 35 m agl (quantum sensor Licor Li-190). Soil heat flux sensors (Huskeflux HFP01SC) are installed at 0.08 m, and soil temperature sensors (thermocouple T-type) are installed at 0.15, 0.2, and 0.5 m below the ground surface.

The postprocessing of the eddy covariance data was done with EddyPro (version 6.0.0, Licor, USA). The raw data were processed in 30-minute block-averaged intervals. The time lag between the wind sensor and the concentration sensor was compensated for, and the WPL term [10] was added. Standard statistical analyses, including spike removal, examination of amplitude resolution test, detection of dropouts and higher-moment statistics in raw data, were performed [11]. For spectral analysis, a high-pass filtering correction according to Moncrieff et al. [12] and a low-pass filtering correction according to Moncrieff et al. [13] were performed. The coordinate system of the 3D ultrasonic anemometer was rotated with the planar fit method [14]. The method was applied to two sectors separately, one for valley breezes and one for mountain breeze situations. The CO_2 profile data were used to derive the storage-term F_S analogously to suggestions given by Aubinet and Chermanne [15].

Gap filling was performed according to Reichstein et al. [16] and by using an online tool which is provided at http://www.bgc-jena.mpg.de/bgi/index.php/Services/REddyProcWeb. The tool includes a friction velocity (u^*) threshold estimation by the moving point test according to Papale et al. [17] and

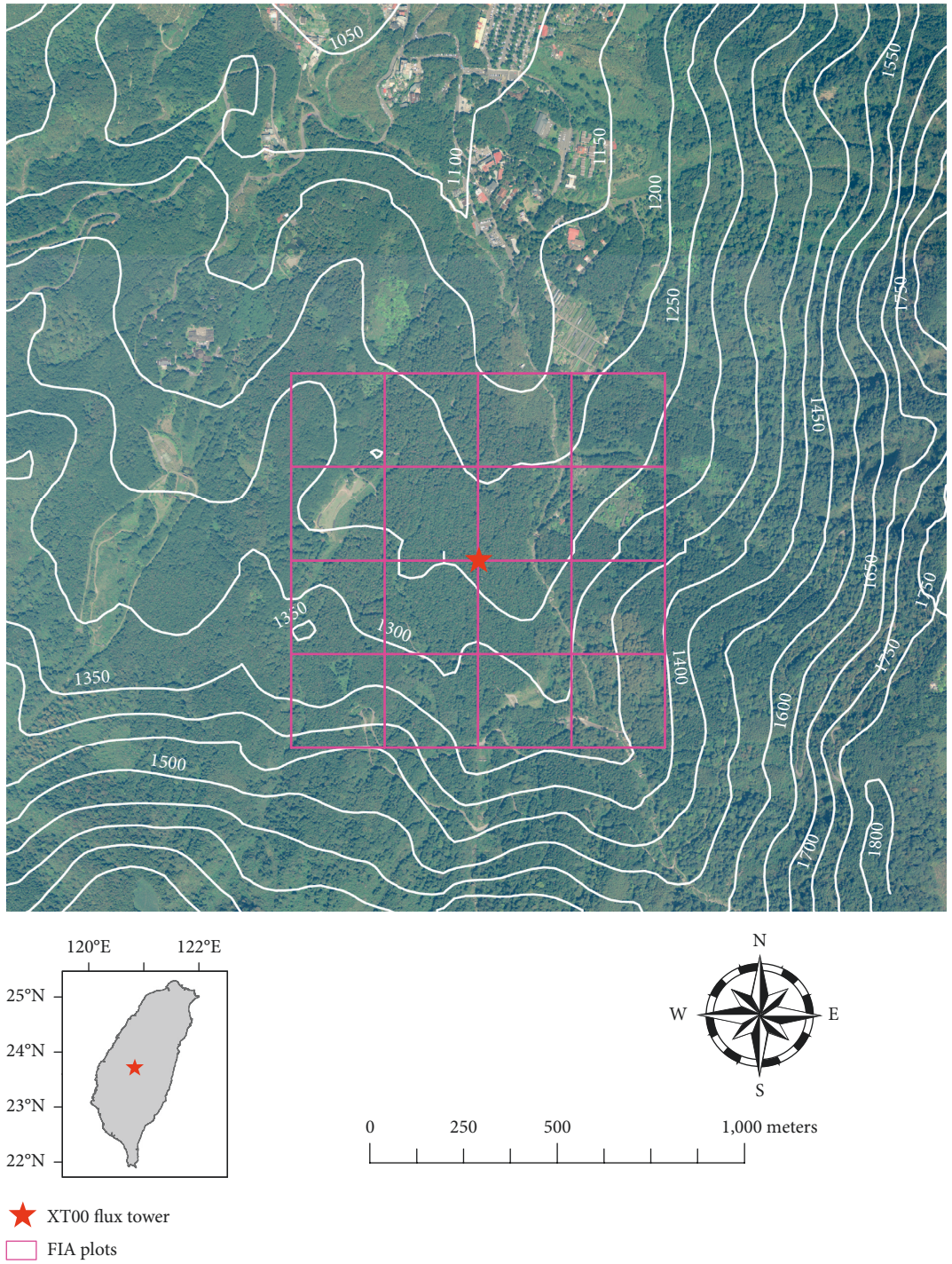

Figure 1: Map of the Xitou area with the location of the eddy covariance tower and the Forest Inventory and Analysis (FIA) plot design (purple squares; plot size 250 × 250 meters).

a night-based flux partitioning algorithm according to Reichstein et al. [16].

2.3. NEE Calculation. The net ecosystem exchange (NEE), as measured with the eddy covariance method, is based on the assumption that the exchange of CO_2 by an ecosystem can be estimated by the sum of the vertical eddy covariance flux (NEE_{EC}) at a specific height and the storage (F_S) between the surface and this height [18]:

$$NEE = NEE_{EC} + F_S. \quad (1)$$

Previous studies found that, during nighttime and under weak mixing conditions, advection cannot be neglected, specifically when the terrain is not flat but has a slope, as in our case [17, 19]. Therefore, the nighttime flux of CO_2 is

likely underestimated as long as the nighttime advection is ignored. The advective term (F_{adv}) cannot be quantified directly with a commonly used eddy covariance system, and there is no standard method to evaluate it properly. We address this issue in a separate paragraph below.

2.4. Quality Assurance. Because of the stand's historic background as a plantation, the trees have a similar height, and the area around the tower is covered with the same species almost throughout. The canopy is closed. From this point of view, the forest is very homogenous and thus the terrain is well suited for application of the eddy covariance technique. The terrain exhibits an even slope with only minor variations in the wind direction both during the nights and during the days and no nearby source of flow disturbance.

For quality classification, an overall quality flag system combining a steady state test and integral turbulence characteristics was applied [20]. Data with low quality were excluded from further analysis. Due to the frequent presence of fog and its obstructive effect on the open-path CO_2 concentration measurement, it was additionally necessary to set an analyser-specific threshold for the AGC value (cleanness indicator of the open-path analyser window) and to exclude all data with an AGC value above this threshold. In the end, it was necessary to exclude the highest and lowest flux results (lower bound quantile 0.3%; upper bound quantile of 99.7%) from further analysis, because disproportionally large flux values (negative and positive) remained in the data. After QA/QC and u^* filtering for $NEE_{EC} + F_S$, 56% of available data for system 1 (70% before u^*-filtering) and 65% of available data for system 2 (79% before u^*-filtering) could be used further. For NEE_{EC} analysis only (ignoring F_s), 54% of the data from system 1 (66% before u^*-filtering) and 61% of the data from system 2 (75% before u^*-filtering) were suitable for further analysis.

Three more tools were employed to review the quality of flux data. First, the energy balance of the surface was checked. The energy balance (E_B) is defined as

$$E_B = R_N - B_S - H - LE, \quad (2)$$

where R_N is the net radiation, B_S the soil heat flux, H is the sensible heat flux, and LE the latent heat flux, which are both as estimated with the eddy covariance method. Generally, the energy balance is not closed (i.e., zero) in forest systems when H and LE are achieved with the eddy covariance method because atmospheric phenomena that cannot be captured with the eddy covariance technique still contribute to a nonperfect closure of the energy balance [18]. A closure of approximately 80% (see method 2 below) has been found for many sites [21, 22]. We conclude that the closure of the energy balance is a helpful indicator of the quality and plausibility of the measured fluxes. If a closure of 80% or more is reached, the measured fluxes are likely of good quality.

Following suggestions given by Wilson et al. [21], we use two methods to evaluate the energy balance closure. The first method includes both linear regression between the half-hourly data of the dependent flux variables H + LE and the independent estimate of $R_N - B_S$ [21]. The second method is the energy balance ratio over all data for each system: the sum of H + LE divided by the sum of $R_N - B_S$. Table 1 shows that, for each method, the degrees of closure between system 1 and system 2 are similar. However, the linear regression method results in a relatively low degree of closure, as compared to 22 FLUXNET sites [21]. Conversely, the energy balance ratio (method 2) shows high degrees of closure: 92% for system 2 and 95% for system 1.

While the energy balance ratio looks promising, it has been shown to have both strengths and weaknesses. McGloina et al. [23] suggested that the energy balance ratio is probably the better indicator for overall degree of energy balance closure at a particular site, because during low closure conditions (e.g., stable stratification), the terms of the E_B function (equation (2)) are usually very low; while the low values of H, LE and R_N have only a small influence on the regression slope, their influence on the energy balance ratio is noticeable. On the other hand, the weakness of the energy balance ratio lies in the fact that biases are prone to be overlooked [21]. Because of advection, as mentioned above, and because of the likely decoupling of turbulence above and below the canopy, as discussed further below, the nighttime fluxes of sensible and latent heat (H and LE) are likely not fully captured by eddy covariance.

Therefore, we presume that the results of the linear regression (method 1) are more reliable and that although the degree of energy balance closure at Xitou is relatively low, it is still within the range of estimates of other sites.

Because the investigated site is located at an inclined surface, there is a difference between the radiation as measured with horizontally aligned radiometers and the amount of radiation reaching the inclined surface. This could have a nonnegligible impact on E_B [23]. While Olmo et al. [24] proposed a correction algorithm for incoming short wave radiation under such conditions, we presume that the correction is hard to realize properly due to the complexity of the terrain (north-facing valley surrounded by higher mountains to the east and south) and due to the high contribution of diffuse radiation resulting from the high frequency of fog. We therefore doubt that such a correction algorithm, which was developed for general applications, will perform well under these circumstances. Further, a correction would lead to a reduction of R_N because the slope is facing north, away from the sun, and the correction would lead to a better agreement between $R_N - B_S$ and H + LE. For these reasons, we refrain from using this correction, and this approach is a conservative one.

The second approach we used to review the quality of flux data (the first was checking the energy balance of the surface) was assessing the relationship between photosynthetic active radiation (PAR) and $NEE_{EC} + F_S$, which is appropriate for examining site-specific data quality. The response of $NEE_{EC} + F_S$ to PAR is very similar for system 1 and system 2 (Figure 2(a)). At no-light conditions, there is no photosynthesis, resulting in a positive $NEE_{EC} + F_S$ flux. With increasing PAR, the ecosystem takes up more and more CO_2 until a maximum uptake is reached. The daily

Table 1: Energy balance closure. Method 1: linear regression between $R_N - B_S$ and H + LE. Method 2: energy balance ratio over all data for each system sum of H + LE divided by $R_N - B_S$.

	Linear regression (method 1)			Energy balance ratio (method 2)
	Slope	Intercept	r^2	%
System 1	0.67	25	0.85	95
System 2	0.68	19	0.89	92

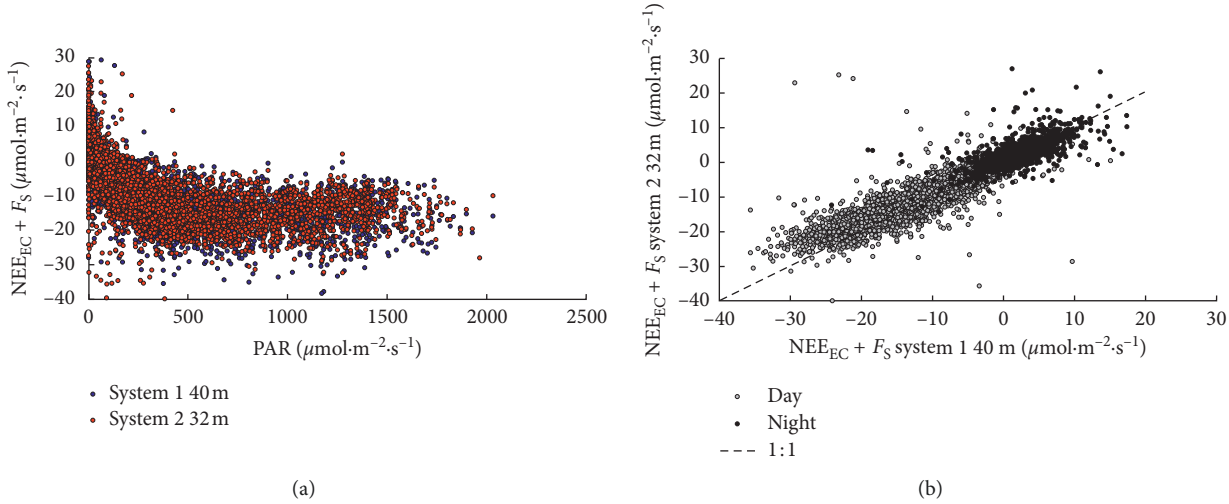

Figure 2: (a) Scatter plot of $NEE_{EC} + F_S$ against PAR; blue symbols show data from system 1 at 40 m agl.; red symbols refer to system 2 at 32 m agl. (b) Scatter plot of $NEE_{EC} + F_S$ system 1 against $NEE_{EC} + F_S$ system 2; black is nighttime data; light grey data points represent daytime data; the black dashed line refers to the 1 : 1 ratio.

mean maximum uptake of all available $NEE_{EC} + F_S$ data is reached at 11:00 a.m. at both systems ($-17\,\mu mol \cdot m^{-2} \cdot s^{-1}$ for system 1 and $-16\,\mu mol \cdot m^{-2} \cdot s^{-1}$ for system 2). Overall, the relationship between $NEE_{EC} + F_S$ shows meaningful flux estimates, except for a few outliers.

In a third approach, we tested the hypothesis that a constant flux layer exists by comparing the results of the two eddy covariance systems at the two heights. The similarity of $NEE_{EC} + F_S$ data for the two systems (which are at different heights) indicates the existence of a constant flux layer. In our data, this is confirmed by the strong correlation between the two data subsets (Figure 2(b)). Note that the relationship between the two systems is stronger during the daytime ($r^2 = 0.80$) than during nighttime ($r^2 = 0.48$).

Overall, all methods employed indicate that the quality of flux data is acceptable even though the site is not located in an ideal environment.

2.5. Advection. It is well accepted that advection is the most common and most important source of errors in eddy covariance applications at night [25]. For mountain and forested sites, the advection issue is particularly important. Especially at nighttime, when turbulence is only weakly developed, phenomena like drainage flow, gravity waves, or even intermittent turbulence may occur and dominate the surface exchange flux [25]. As these phenomena cannot be captured by the eddy covariance measurement, systematic errors may arise when estimating NEE from it. There are different methods for taking into account the influence of weak mixing and the advective flux (F_{adv}) contribution. The most common method is the u^*-filtering approach. Here, a u^* threshold is estimated for the detection of periods when nighttime NEE ($NEE_{EC} + F_S$) becomes sensitive to u^* [17, 19]. Because nighttime flux should be independent of u^*, any dependence should arise from an artefact. In consequence, the periods with u^* values below the threshold, i.e., when NEE is sensitive to u^*, are filtered out. Nonetheless, whether or not the u^*-filtering approach is suitable as a standard quality assurance technique is still controversially discussed [22, 26].

An alternative to the u^* method is given by van Gorsel et al. [27]. They found for different sites that peaks of $NEE_{EC} + F_S$ (defined as R_{max}) occurred during the early evenings and before the full development of the advective processes that lead to an underestimation of the nighttime CO_2 fluxes. They used R_{max} to derive a temperature response function for respiration and eventually an estimate of the nighttime respiration. The results of this method fit well with those of other methods (like independent chamber measurements), and van Gorsel et al. showed that it works for forest sites as well. This method is applicable when storage data is available and if the early-evening peak in $NEE_{EC} + F_S$ occurs.

At the Xitou site, the early-evening peak occurs only during 7 out of 15 months with storage data. During the winter months (except for November 2011), no peak occurred. As the wind direction changes regularly from valley breeze to mountain breeze in the early evenings, these

respective transition periods are associated with low wind speeds and low u^*. Further, the quality control requirements of the van Gorsel method reduce the number of available data points at the Xitou site, leading to an unusually high, yet not well documented, peak in September 2013. Overall, our evaluation is in line with the presumption of van Gorsel et al. that complex flow patterns limit the applicability of their approach [27]. For these reasons and for the sheer absence of storage data for large portions of our data set, the van Gorsel method is not useful in this case to estimate yearly carbon balances. In the supplement material, the daily course of each available month of $NEE_{EC} + F_S$ data for system 2 is shown together with the results of the later-described estimate of day-based respiration.

There are also studies which attempt to solve the nighttime advection problem by measuring the advection flux directly. With great effort, Aubinet et al. [28] were able to directly measure advection, but they came to the conclusion that it does not help to solve the nighttime problem. The main problem they identified was that the experimental approach to measure the advection flux was insufficient in terms of spatial representativeness. This led to systematic errors that probably cannot be solved at all [28]. Thomas et al. [26] designed a method to measure the submeso motions below the canopy and to compensate for the advective losses in this way. This method includes eddy covariance measurements below the canopy; however, these measurements are not available at the Xitou site for the experimental period.

To test the data sets for the presence and potential importance of advection fluxes, we use, as a first step, the u^*- filtering method as employed in the gap-filling tool with storage-corrected eddy flux data ($NEE_{EC} + F_S$). The storage term F_S can influence the estimation of the u^* threshold [17]; therefore, it is important to perform the storage correction before u^* threshold estimation. The gap-filling tool identified u^* thresholds between 0.08 and 0.14 $m \cdot s^{-1}$ (0.1 and 0.16 $m \cdot s^{-1}$ without F_S term) for system 1 and system 2, respectively. If a u^* value was below the specific threshold, the corresponding flux value was marked as gap. Overall, 14% of the flux data for each eddy system was marked as a gap because of low u^*. At night, the proportion of data filtered out through the u^* threshold exceeds 25%.

To test whether the u^* filtering approach worked and periods affected by advection were fully excluded, we used two different approaches for partitioning the gap-filled, u^*-filtered $NEE_{EC} + F_S$ data to evaluate ecosystem respiration R_E. First, we used the night-based flux partitioning approach included in the employed gap-filling tool [16]. This sets the nighttime NEE data as R_E and extrapolates this data with the exponential regression model by Lloyd and Taylor [29] to the daytime. In the following, we refer to this approach as night-based respiration R_{E_NB}. Detailed information is given in [16, 30].

Second, we combined one of the day-based approaches (DB all no VPD—all parameters estimated using daytime data, no consideration of vapor pressure deficit (VPD)) of Lasslop et al. [31] with the technique used by Lee et al. [32]. The daytime approach is based on the relationship between the photosynthetically active radiation and the estimated $NEE_{EC} + F_S$. In this model, NEE is described by a combination of the hyperbolic light-response curve [33] and the Lloyd and Taylor model:

$$\mathrm{NEE} = \frac{\alpha\beta\mathrm{PAR}}{\alpha\mathrm{PAR} + \beta} + rb \exp\left(E_0\left(\frac{1}{T_{\mathrm{ref}} - T_0} - \frac{1}{T - T_0}\right)\right). \quad (3)$$

The daytime model was fed only with radiation data with $\mathrm{PAR} > 10\,\mu\mathrm{mol} \cdot m^{-2} \cdot s^{-1}$. T_0 and T_{ref} were fixed to the same values as they were in the night-based approach. For T, the air or soil temperatures need to be known. This model was used with a 15-day moving window with the actual day in the middle of the window [32]. The coefficients α, β, rb, and E_0 (Equation (3)) were estimated with a nonlinear curve-fitting method (trust-region-reflective algorithm). The model was quality controlled analogously to suggestions given by Lasslop et al. [31]. The coefficients rb and E_0, as estimated with daytime data, were then used to calculate the day-based respiration R_{E_DB} with the second term on the right-hand side of Equation (3). If the site is not affected or is only a little affected by advection and if the u^* filtering is working properly, the two models should yield similar results.

It is important which temperature (soil or air) is employed for the respective models. Air temperature (T_{air}) is used for both models because the sums of squares between the employed modeling function T_{air} with $NEE_{EC} + F_S$ were better than those between soil temperature and $NEE_{EC} + F_S$. In addition, the physical distance between the anemometer and the soil is large, and the canopy is located between these levels, meaning that a strong correlation between the soil temperature and $NEE_{EC} + F_S$ is not likely to occur.

3. Results and Discussion

Profiles of meteorological parameters and CO_2 concentrations at the tower provide insight into the exchange processes between the air masses above the forest canopy, within the trunk space, and at the soil-surface interface. In Figure 3, median wind speeds and wind directions are shown for different heights within the forest and above the canopy. The median wind speed was generally higher at all heights during nighttime than during the days. There was little diurnal variation of the median wind speed only at the canopy height of 25 m agl. The median wind speed exhibited a minimum in the upper heights during the day, when the wind direction changed in the morning and afternoon. During nighttime, the median wind speed within the denser canopy at 18 m agl and at 25 m agl was lower than in the more open trunk space at 6 m agl. In daytime, when the valley wind was established, there was almost no difference in the median wind speeds at the levels within and below the canopy (25 m, 18 m, and 6 m agl).

The wind direction changed both above and below the canopy due to the valley wind regime. During the mornings, a valley wind developed. The respective change of the

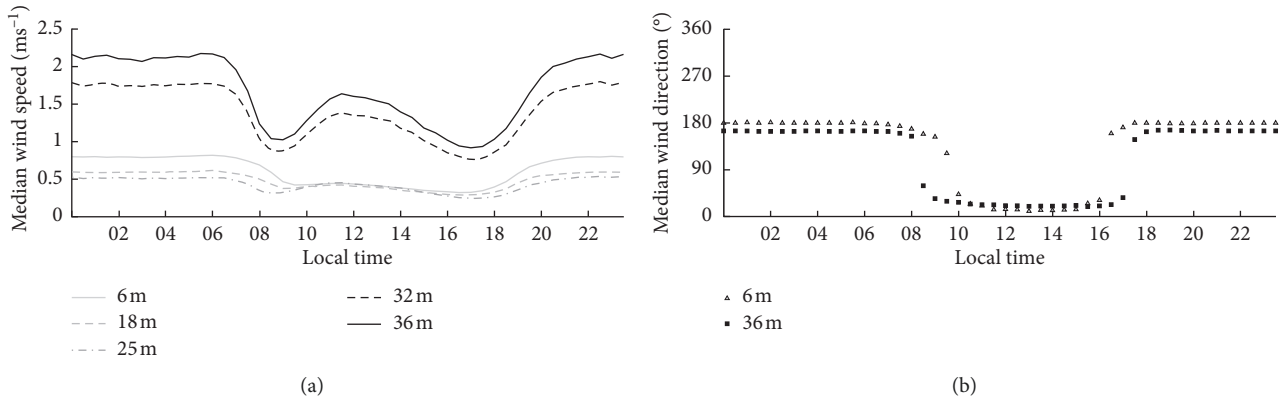

Figure 3: Median wind speed and median wind direction at different heights.

median wind direction occurred first above the canopy (36 m agl), and then the change happened about one hour later under the canopy (6 m agl). Interestingly, the change from the valley wind (northerly directions) to the mountain wind (southerly directions) in the evenings happened about an hour earlier under the canopy than above it. The temperature profile (not shown) indicates that, in the morning, the air above the canopy heats up earlier than under the canopy, which supports the earlier formation of the valley breeze above the canopy. In the evening, the air under the canopy cools down before the air above, which leads to an earlier downward flow. Note that during nighttime, the wind speed below and above the canopy were higher than during daytime, whereas the wind speed within the canopy differed little between day and night. This strongly indicates that vertical exchange through the canopy is inhibited during the night.

For further insights, we analyzed CO_2 profile data. The CO_2 profile data are available for 2011 (September to December), 2012 (August to December, 84% data), and 2013 (full year). The median CO_2 mixing ratio (Figure 4) shows a well-mixed situation during the days with similar CO_2 mixing ratios throughout almost the entire vertical profile. During nighttime, CO_2 apparently accumulates under the canopy and near the ground.

Combining the wind speed, wind direction, and CO_2 profiles, there are two regimes, which indicate the presence of two separate situations regarding the NEE estimate. In the daytime, the radiation-induced convective processes lead to a mixing of air masses between the layer above the canopy and the trunk space. The air between the soil surface and the eddy systems is well mixed then. During the second situation at night, when the wind direction has changed (or when it is just changing) and a stably stratified boundary layer is being established, there is probably little or no interaction between the flux above the canopy and below. Under these conditions, the canopy builds a barrier that cannot be overcome by mechanically induced turbulence. As a result, the nighttime respiration flux under the canopy is not detected by the eddy covariance system above the canopy. During these times, the respirated CO_2 is not only stored under the canopy (Figure 4) but also transported away by drainage flow, thus bypassing the eddy systems above. We conclude that an unknown amount of respiration flux must be missing in the NEE if it is calculated as u^* corrected $NEE_{EC} + F_S$ during nighttime.

3.1. Comparing R_{E_DB} and R_{E_NB}. Table 2 and Figure 5 show the results of the night-based and the day-based models to estimate ecosystem respiration from $NEE_{EC} + F_S$ data. For $NEE_{EC} + F_S$ data, this comparison could be computed only for a total of 10 months for system 1 and 15 months for system 2 in the period 2011–2013, because profile data are not available for other periods.

Figure 5(b) shows, as an example, the mean daily course of R_E estimates for system 2. The overall mean of the night-based respiration model (R_{E_NB}) for system 2 is 2.2 μmol·m^{-2}·s^{-1} (2.4 μmol·m^{-2}·s^{-1} system 1, not shown in detail). For the day-based partitioning (R_{E_DB}), it is 4.6 μmol·m^{-2}·s^{-1} (4.4 μmol·m^{-2}·s^{-1} system 1). The Figure 5(a) shows the correlations between air temperature and ecosystem respiration. The minimum of the daily mean air temperature was 6.0°C. The corresponding respiration for system 2 is 1.0 μmol·m^{-2}·s^{-1} R_{E_NB} (0.87 μmol·m^{-2}·s^{-1} system 1) and 3.4 μmol·m^{-2}·s^{-1} R_{E_DB} (3.2 μmol·m^{-2}·s^{-1} system 1). The maximum of the daily mean air temperature in the analyzed period was 22°C. The corresponding respiration values for system 2 are 3.0 μmol·m^{-2}·s^{-1} R_{E_NB} (3.6 μmol·m^{-2}·s^{-1}system 1) and 6.9 μmol·m^{-2}·s^{-1} R_{E_DB} (6.6 μmol·m^{-2}·s^{-1} system 1). Table 2 shows the sums of the various R_E model results. The average monthly sums are similar for system 1 and system 2. The estimate of R_{E_DB} is about twice as high as that for R_{E_NB}. This also holds for the hourly median values and the monthly sums.

If there is no or little advection, the results of these models should be similar. Because of the huge differences in the R_E estimations and the described meteorological situation, we presume that, at Xitou, NEE cannot be estimated by $NEE_{EC} + F_S$ only. Our assumption is that during nighttime, the eddy covariance system above the forest and the estimation of the storage cannot detect the full respiration of the forest. Further, the u^* filtering alone does not avoid incorrect nighttime data.

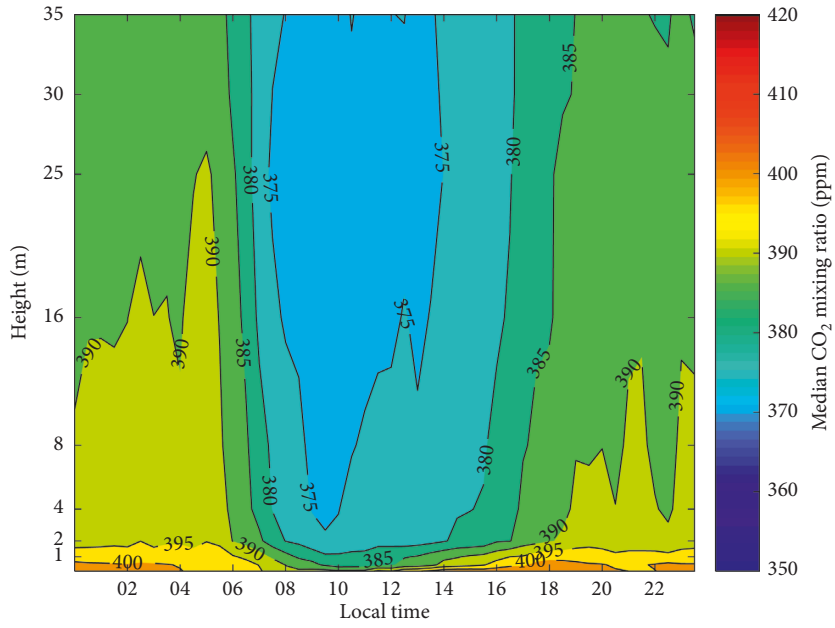

Figure 4: Median CO_2 mixing ratios in ppm at different heights.

Table 2: Ecosystem respiration (R_E) from the nighttime and the daytime partitioning models R_{E_NB} and R_{E_DB}, respectively. Monthly sums represent times when complete gap-filled data sets are available (available months indicated in brackets).

$g \cdot C \cdot m^{-2}$ per time unit	System 1		System 2	
	R_{E_NB}	R_{E_DB}	R_{E_NB}	R_{E_DB}
2011				
System 1 (10, 11)	144	303	126	289
System 2 (10, 11)				
2012				
System 1 (-)	—	—	233	614
System 2 (9–12)				
2013				
System 1 (2–4; 8–12)	562	1,157	652	1,249
System 2 (1–4; 8–12)				
Average monthly sums	71	146	67	144

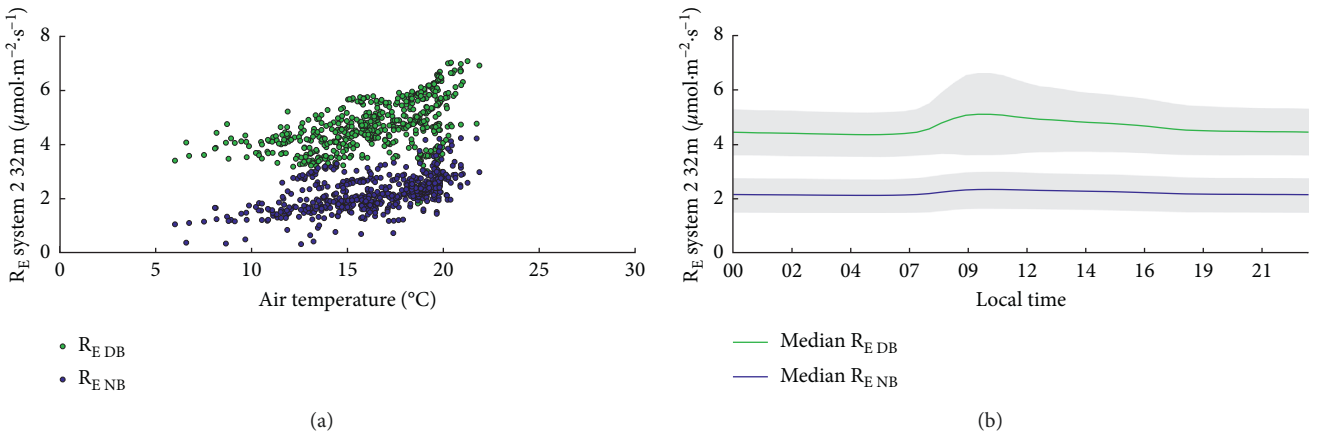

Figure 5: (a) Scatter plot of daily mean R_E system 2 against daily mean air temperature; green symbols show data for the daytime partitioning model R_{E_DB}; blue symbols show data for the nighttime partitioning model R_{E_NB}. (b) Median daily course of R_{E_DB} and R_{E_NB} for system 2; grey areas indicate one standard deviation.

3.2. Advanced Methodology to Estimate NEE. In the quality assurance section above, we showed that this site is, in principle, suitable for the application of the eddy covariance technique even though it is located in not ideal heterogenic topography. It was also shown that advection cannot be neglected. In order to develop an advanced estimate of the NEE, we combine the measured NEE_{EC} and the results of the day-based partitioning approach.

However, it is necessary to evaluate the influence of the storage term. We compare the storage-corrected and not-storage-corrected gap-filled fluxes with the u^*-filtered NEE. A linear regression (not shown in detail) shows a strong relationship between NEE_{EC} and $NEE_{EC} + F_S$ with $r^2 = 0.98$ for system 1 and $r^2 = 0.97$ for system 2. The summed-up flux of system 1 shows almost identical results for storage-corrected and not-storage-corrected fluxes. For system 2, the summed-up storage-corrected fluxes are 1% lower than the fluxes without storage correction. Note that, for system 1, there are no respective data available for 2012. In addition, the storage data of 2011 and 2012 are only available for the last months of these years. It cannot be excluded that for a full data set, the storage term might have a bigger influence on the monthly and yearly sum of NEE. Nevertheless, because of missing profile measurements and because the contribution of storage is limited, we ignore this term during further analysis in order to achieve an estimate for the whole NEE_{EC} data set.

Based on the presumption that the nighttime NEE_{EC} data need to be corrected, we arrive at NEE_X, which is an advanced estimate of NEE at the Xitou site. NEE_X for every half hour is defined as

$$NEE_X = \begin{cases} NEE_{EC}, & \text{not mountain breeze} \\ NEE_{DB}, & \text{mountain breeze} \end{cases}, \quad (4)$$
$$NEE_{DB} = NEE_{EC} - R_{E\_NB} + R_{E\_DB}.$$

For a mountain breeze (wind directions 135°–225°), NEE is defined as NEE_{DB}. During the changes of the wind regime and during valley winds (wind directions 315°–45°), NEE is defined as NEE_{EC}. For gap-filling purposes, the missing wind direction data are defined as the weekly or monthly means for each half hour. Missing data were primarily filled with the weekly means of the missing half hours; only in cases when no weekly mean data points were available for gap filling were the gaps filled with the monthly means.

3.3. Results of NEE Estimate. Table 3 lists the results of the nighttime and daytime partitioning approaches and the NEE estimates including the daytime respiration. Negative NEE values indicate carbon uptake.

The results of R_{E_DB} shown in Table 3 are (like in Table 2) nearly twice as high as the results for R_{E_NB}. The results of the R_{E_NB} estimate, with a range from 938 to 1,038 $g{\cdot}C{\cdot}m^{-2}{\cdot}y^{-1}$, seem very low for this kind of ecosystem, whereas the results of R_{E_DB} (1,754 to 1,961 $g{\cdot}C{\cdot}m^{-2}{\cdot}y^{-1}$) are more reasonable. As a consequence of low R_{E_NB}, the estimate of NEE_{EC} is highly negative ranging from −1,027 to −1,101 $g{\cdot}C{\cdot}m^{-2}{\cdot}y^{-1}$. Based on the estimate given in Equation (4), the magnitude of NEE is reduced to a range from −434 to −652 $g{\cdot}C{\cdot}m^{-2}{\cdot}y^{-1}$ (NEE_X) with an average of −561 $g{\cdot}C{\cdot}m^{-2}{\cdot}y^{-1}$.

Table 4 presents results of NEE estimates at forest sites comparable to ours. For a subtropical mountain forest with frequent occurrence of fog like at Xitou, central Taiwan, there are only a few studies representing a similar ecosystem of forest sites. Therefore, a number of studies from Japan with a more temperate climate are included for comparison (Table 4).

Table 4 lists a number of comparable studies with NEE and R_E estimates and results of the increase of live-tree biomass evaluated with independent forest inventory methods. The largest NEE estimate found is by Tan et al. [34] with about −900 $g{\cdot}C{\cdot}m^{-2}{\cdot}yr^{-1}$. Tan et al. [34] identified two potential drivers for the large carbon uptake found at their study site. First, the low temperature at the high-altitude site may have reduced the respiration, and secondly, the high proportion of indirect, diffuse solar radiation due to the extended presence of clouds may have enhanced photosynthesis. In the other studies, the NEE ranges between −330 and −630 $g{\cdot}C{\cdot}m^{-2}{\cdot}yr^{-1}$. The respective respiration rates R_E range between 991 and 3061 $g{\cdot}C{\cdot}m^{-2}{\cdot}y^{-1}$.

If we compare our results to those of these other studies, the estimates of NEE_X and R_{E_DB} (−561 and 1,828 $g{\cdot}C{\cdot}m^{-2}{\cdot}yr^{-1}$, respectively) seem reasonable. It is evident that the more direct estimates NEE_{EC} and R_{E_NB} (−1,060 and 983 $g{\cdot}C{\cdot}m^{-2}{\cdot}yr^{-1}$) provide no valid estimates of the forest-atmosphere exchange at the Xitou site. Further, the estimate for the mean increment in live-tree biomass in the direct vicinity of the flux tower (560 $g{\cdot}C{\cdot}m^{-2}{\cdot}yr^{-1}$; mean 2011–2017; interpolated data) and the estimate of Cheng et al. [38] (265 $g{\cdot}C{\cdot}m^{-2}{\cdot}yr^{-1}$) for the whole Xitou area are in rather good agreement to the NEE_X estimates. Yu et al. [39] estimated an annual soil respiration of 1,003 $g{\cdot}C{\cdot}m^{-2}{\cdot}yr^{-1}$ derived from monthly data at Xitou in 2012. They used automated chamber systems, which operate independently of the eddy covariance method. A comparison of this estimate of soil respiration only with R_{E_NB} of the entire ecosystem (938 $g{\cdot}C{\cdot}m^{-2}{\cdot}yr^{-1}$ in 2012) again leads to the presumption that R_{E_NB} does not fully capture the ecosystem respiration. R_{E_NB} should be larger than the soil respiration because it also includes the respiration of the above-ground vegetation. It is reasonable to assume that this discrepancy applies to years other than 2012 as well. The listed data support our understanding that the NEE cannot be estimated with u^*-corrected NEE_{EC} data at the Xitou site. Due to the fact that the contribution of the storage term F_S is limited, NEE cannot be estimated by u^*-corrected $NEE_{EC} + F_S$ either. In essence, NEE_X is the best estimate for the net ecosystem exchange flux (NEE) at the Xitou site.

4. Conclusions

This study analyzed CO_2 flux data of a subtropical mountain forest site in central Taiwan from 2011 through 2013. The analysis of the local wind regime and a detailed study of NEE and R_E estimates, based on various partitioning models fed with u^* and storage-corrected flux data, provided evidence

Table 3: Yearly ecosystem respiration (R_E) from the nighttime (gap-filling tool) and daytime (Equation (3)) partitioning models; net ecosystem exchange defined as NEE_{EC} after QA/QC, gap filling and u^* filtering; net ecosystem exchange including NEE_{DB} for mountain breeze (NEE_X based on equation (4)).

$g \cdot C \cdot m^{-2} \cdot yr^{-1}$	System 1				System 2			
	R_{E_NB}	R_{E_DB}	NEE_{EC}	NEE_X	R_{E_NB}	R_{E_DB}	NEE_{EC}	NEE_X
2011	972	1,754	−1,102	−652	—	—	—	—
2012	—	—	—	—	938	1,961	−1,027	−434
2013	—	—	—	—	1,038	1,769	−1,051	−598

Table 4: Yearly sums of NEE and R_E from this study and other studies. Estimates of yearly live-tree biomass with forest inventory methods (positive values represent carbon sequestration) around the flux tower and in the whole Xitou area. Numbers in parentheses are single standard deviations.

Reference	NEE $g \cdot C \cdot m^{-2} \cdot yr^{-1}$	R_E
This study: mean 2011–2013	NEE_{EC} = −1,060 (±38) NEE_X = −561 (±114)	R_{E_NB} = 983 (±51) R_{E_DB} = 1,828 (±115)
Tan et al. [34] quantify the carbon uptake of a 300-year-old subtropical evergreen broadleaved forest	~−900	—
Yu et al. [4], East Asian monsoon region	−362 (±39)	—
Takanashi et al. [35], Japanese cedar forest in Japan 2001 and 2002 [35]	−477, −480	991, 1,129
Saitoh et al. [36], mostly Japanese cedar and Japanese cypress forest in Japan; 2006 and 2007	−330, −350	1,740, 1980
Kosugi et al. [37] analyse 7 years of data; 50-year-old forest consisting Japanese cypress (method 1-> night-based gap-filling; method 2-> day-based gap filling)	m1 = −490 m2 = −630	m1 = 1,555 m2 = 1,554
Luyssaert et al. [3], combining 29 tropical humid evergreen forest sites	−403 (±102)	3061 (±56)
	Yearly increase in live-tree biomass ($g \cdot C \cdot m^{-2} \cdot yr^{-1}$)	
Forest biomass survey in Xitou Forest inventroy and analysis (FIA) plot design; mean of 4 plots from 2011–2017 linear interpolated	560	—
Cheng et al. [38], forest inventory methods, complete analysis of Xitou area	265	—

of a large underestimate of the positive nighttime fluxes. Advection is a strong player at this site. Below-canopy drainage flow leads to a net downhill transport of CO_2 from nighttime respiration. This process cannot be detected by the eddy covariance systems above the canopy because there is an effective nighttime decoupling of air masses below the canopy from those above. When using a day-based partitioning model for the whole data set of NEE_{EC} data, we arrived at an improved estimate of the carbon uptake of the forest (Equation (4)). According to our estimate, NEE_X is −561 (±114) $g \cdot C \cdot m^{-2} \cdot yr^{-1}$ (±one standard deviation). The mean increment of live-tree biomass in the direct neighbourhood of the tower was estimated to be 560 $g \cdot C \cdot m^{-2} \cdot yr^{-1}$ (mean 2011–2017; interpolated data). Consequently, the growth of above-ground live-tree biomass is the main factor for carbon taken up by the forest. We trust that this estimate of the yearly carbon uptake is the best that can be achieved with the available data sets. The use of several flux partitioning models for the purpose of quality assurance proved to be a helpful approach to quantify the yearly flux estimates at the mountain forest site under study. Nonetheless, the remaining uncertainty is hard to quantify. It is planned to compare this approach with other methods like those proposed by Thomas et al [26], which require additional eddy covariance measurements within the trunk space.

Data Availability

The data used to support the findings of this study are available from the corresponding author upon request.

Conflicts of Interest

The authors declare that there are no conflicts of interest regarding the publication of this paper.

Acknowledgments

We thank Celeste Brennecka for language editing. The provision of travel funds from the German Academic Exchange Service (DAAD) through funds of the German Federal Ministry of Education and Research (BMBF), the Taiwanese funds from the Ministry of Science and Technology (MOST) under Grant 105-2911-I-002-529-MY2, and

Experimental Forest, National Taiwan University, are all gratefully acknowledged.

Supplementary Materials

An overview about the van Gorsel method. (*Supplementary Materials*)

References

[1] G. Bonan, "Forests and climate change: forcings, feedbacks, and the climate benefits of forests," *Science*, vol. 320, no. 5882, pp. 1444–1449, 2008.

[2] FLUXNET, *FLUXNET—Global Network of Micrometeorological Tower Sites that Use Eddy Covariance*, 2018, https://fluxnet.ornl.gov/.

[3] S. Luyssaert, I. Inglima, M. Jung et al., "CO_2 balance of boreal, temperate, and tropical forests derived from a global database," *Global Change Biology*, vol. 13, no. 12, pp. 2509–2537, 2007.

[4] G. Yu, Z. Chen, S. Piao et al., "High carbon dioxide uptake by subtropical forest ecosystems in the East Asian monsoon region," *Proceedings of the National Academy of Sciences*, vol. 111, no. 13, pp. 4910–4915, 2014.

[5] K. Mildenberger, E. Beiderwieden, Y.-J. Hsia, and O. Klemm, "CO_2 and water vapor fluxes above a subtropical mountain cloud forest-the effect of light conditions and fog," *Agricultural and Forest Meteorology*, vol. 149, no. 10, pp. 1730–1736, 2009.

[6] T. S. El-Madany, H. F. Duarte, D. J. Durden et al., "Low-level jets and above-canopy drainage as causes of turbulent exchange in the nocturnal boundary layer," *Biogeoscience*, vol. 11, no. 16, pp. 4507–4519, 2014.

[7] D. Baldocchi, "Assessing the eddy covariance technique for evaluating carbon dioxide exchange rates of ecosystems: past, present and future," *Global Change Biology*, vol. 9, no. 4, pp. 479–492, 2003.

[8] Y.-L. Liang, T.-C. Lin, J.-L. Hwong, N.-H. Lin, and C.-P. Wang, "Fog and precipitation chemistry at a mid-land forest in central Taiwan (in Chinese with english abstract)," *Journal of Environment Quality*, vol. 38, no. 2, pp. 627–636, 2009.

[9] T. H. Wey, Y. J. Lai, C. S. Chang et al., "Preliminary studies on fog characteristics at Xitou region of central Taiwan," *Journal of the Experimental Forest of National Taiwan University*, vol. 25, pp. 149–160, 2011.

[10] E. K. Webb, G. I. Pearman, and R. Leuning, "Correction of flux measurements for density effects due to heat and water vapor transfer," *Quarterly Journal of the Royal Meteorological Society*, vol. 106, no. 447, pp. 85–100, 1980.

[11] D. Vickers and L. Mahrt, "Quality control and flux sampling problems for tower and aircraft data," *Journal of Atmospheric and Oceanic Technology*, vol. 14, no. 3, pp. 512–526, 1997.

[12] J. B. Moncrieff, R. Clement, J. Finnigan, and T. Meyers, "Averaging, detrending and filtering of eddy covariance time series," in *Handbook of Micrometeorology: A Guide for Surface Flux Measurements*, pp. 7–13, Springer Science & Business Media, Berlin, Germany, 2004.

[13] J. Moncrieff, J. Massheder, H. deBruin et al., "A system to measure surface fluxes of momentum, sensible heat, water vapour and carbon dioxide," *Journal of Hydrology*, vol. 188-189, pp. 589–611, 1997.

[14] J. Wilczak, S. Oncley, and S. Stage, "Sonic anemometer tilt correction algorithms," *Boundary-Layer Meteorology*, vol. 99, no. 1, pp. 127–150, 2001.

[15] M. Aubinet and B. Chermanne, "Long term carbon dioxide exchange above a mixed forest in Belgium," *Agricultural and Forest Meteorology*, vol. 108, no. 4, pp. 293–315, 2001.

[16] M. Reichstein, E. Falge, and D. Baldocchi, "On the separation of net ecosystem exchange into assimilation and ecosystem respiration: review and improved algorithm," *Global Change Biology*, vol. 11, no. 9, pp. 1424–1439, 2005.

[17] D. Papale, M. Reichstein, M. Aubinet et al., "Towards a standardized processing of net ecosystem exchange measured with eddy covariance technique: algorithms and uncertainty estimation," *Biogeoscience*, vol. 3, no. 4, pp. 571–583, 2006.

[18] T. Foken, R. Leuning, S. R. Oncley, M. Mauder, and M. Aubinet, "Corrections and data quality control," in *Eddy Covariance—A Practical Guide to Measurement and Data Analysis*, pp. 85–131, Springer Science & Business Media, Berlin, Germany, 2012.

[19] M. Goulden, J. Munger, S. Fan, B. Daube, and S. Wofsy, "Measurements of carbon sequestration by long-term eddy covariance: methods and a critical evaluation of accuracy," *Global Change Biology*, vol. 2, no. 3, pp. 169–182, 1996.

[20] M. Mauder and T. Foken, *Documentation and Instruction Manual of the Eddy-Covariance Software Package TK3*, 2004, https://epub.uni-bayreuth.de/342/1/ARBERG046.pdf.

[21] K. Wilson, A. Goldstein, E. Falge et al., "Energy balance closure at FLUXNET sites," *Agricultural and Forest Meteorology*, vol. 113, no. 1–4, pp. 223–243, 2002.

[22] T. Foken, F. Meixner, E. Falge et al., "Coupling processes and exchange of energy and reactive and non-reactive trace gases at a forest site results of the EGER experiment," *Atmospheric Chemistry and Physics*, vol. 12, no. 4, pp. 1923–1950, 2012.

[23] R. McGloina, L. Šiguta, K. Havránkováa, J. Dušeka, M. Pavelkaa, and P. Sedláka, "Energy balance closure at a variety of ecosystems in Central Europe with contrasting topographies," *Agricultural and Forest Meteorology*, vol. 248, pp. 418–431, 2018.

[24] F. Olmo, J. Vida, I. Foyo, Y. Castro-Diez, and L. Alados-Arboledas, "Prediction of global irradiance on inclined surfaces from horizontal global irradiance," *Energy*, vol. 24, no. 8, pp. 689–704, 1999.

[25] M. Aubinet, "Eddy covariance CO_2 flux measurements in nocturnal conditions: an analysis of the problem," *Ecological Applications*, vol. 18, no. 6, pp. 1368–1378, 2008.

[26] C. Thomas, J. G. Martin, B. E. Law, and K. Davis, "Toward biologically meaningful net carbon exchange estimates for tall: multi-level eddy covariance canopy coupling regimes in a mature Douglas fir forest Oregon," *Agricultural and Forest Meteorology*, vol. 173, pp. 14–27, 2013.

[27] E. van Gorsel, N. Delpierre, R. Leuning et al., "Estimating nocturnal ecosystem respiration from the vertical turbulent flux and change in storage of CO_2," *Agricultural and Forest Meteorology*, vol. 149, no. 11, pp. 1919–1930, 2009.

[28] M. Aubinet, C. Feigenwinter, B. Heinesch et al., "Direct advection measurements do not help to solve the night-time CO_2 closure problem: evidence from three different forests," *Agricultural and Forest Meteorology*, vol. 150, no. 5, pp. 655–664, 2010.

[29] J. Lloyd and J. Taylor, "On the temperature dependence of soil respiration," *Functional Ecology*, vol. 8, no. 3, pp. 315–323, 1994.

[30] M. P. I. f. Biogeochemistry, *Data Products, Online Services & Open Software*, 2018, https://www.bgc-jena.mpg.de/bgi/index.php/Services/Overview.

[31] G. Lasslop, M. Reichstein, D. Papale et al., "Separation of net ecosystem exchange into assimilation and respiration using a light response curve approach: critical issues and global evaluation," *Global Change Biology*, vol. 16, no. 1, pp. 187–208, 2010.

[32] X. Lee, J.-D. Fuentes, R. Staebeler, and H. Neumann, "Long-term observation of the atmospheric exchange of CO_2 with a temperate deciduous forest in southern Ontario, Canada," *Journal of Geophysical Research: Atmospheres*, vol. 104, no. 13, pp. 15975–15984, 1999.

[33] E. Falge, D. Baldocchi, and R. Olson, "Gap filling strategies for defensible annual sums of net ecosystem exchange," *Agricultural and Forest Meteorology*, vol. 107, no. 1, pp. 43–69, 2001.

[34] Z.-H. Tan, Y.-P. Zhang, D. Schaefer, G.-R. Yu, N. Liang, and Q.-H. Song, "An old-growth subtropical Asian evergreen forest as a large carbon sink," *Atmospheric Environment*, vol. 45, no. 8, pp. 1548–1554, 2011.

[35] S. Takanashi, Y. Kosugi, Y. Tanaka et al., "CO_2 exchange in a temperate Japanese cypress forest compared with that in a cool-temperate deciduous broad-leaved forest," *Ecological Research*, vol. 20, no. 3, pp. 313–324, 2005.

[36] T. M. Saitoh, I. Tamagawa, H. Muraoka, N.-Y. M. Lee, Y. Yashiro, and H. Koizumi, "Carbon dioxide exchange in a cool-temperate evergreen coniferous forest over complex topography in Japan during two years with contrasting climates," *Journal of Plant Research*, vol. 123, no. 4, pp. 473–483, 2010.

[37] Y. Kosugi, S. Takanashi, M. Ueyama et al., "Determination of the gas exchange phenology in an evergreen coniferous forest from 7 years of eddy covariance flux data using an extended big-leaf analysis," *Ecological Research*, vol. 28, no. 3, pp. 373–385, 2013.

[38] C.-H. Cheng, C.-Y. Hung, C.-P. Chen, and C.-W. Pei, "Biomass carbon accumulation in aging Japanese cedar plantations in Xitou, central Taiwan," *Botanical Studies*, vol. 54, no. 1, p. 60, 2013.

[39] J. Yu, Y. Lai, P. Chiang, N. Liang, Y. Wang, and C. Horng, "Soil respiration dynamic in subtropical old-plantation forest," in *Proceedings of International Conference on Global Changes, Forest Adaption and CO_2 Flux Monitoring*, Islamabad, Pakistan, May 2012.